ACS APPLIED MATERIALS & INTERFACES
Research Article
www.acsami.org

Photochemical Charge Separation at Particle Interfaces: The n-$BiVO_4$−p-Silicon System

Yuxin Yang,[†,‡] Jiarui Wang,[‡] Jing Zhao,[‡] Benjamin A. Nail,[‡] Xing Yuan,[†] Yihang Guo,[†] and Frank E. Osterloh*[,‡]

[†]School of Environment, Northeast Normal University, Changchun 130117, P.R. China

[‡]Department of Chemistry, University of California, Davis, California 95616, United States

Supporting Information

ABSTRACT: The charge transfer properties of interfaces are central to the function of photovoltaic and photoelectrochemical cells and photocatalysts. Here we employ surface photovoltage spectroscopy (SPS) to study photochemical charge transfer at a p-silicon/n-$BiVO_4$ particle interface. Particle films of $BiVO_4$ on an aluminum-doped p-silicon wafer were obtained by drop-coating particle suspensions followed by thermal annealing at 353 K. Photochemical charge separation of the films was probed as a function of layer thickness and illumination intensity, and in the presence of methanol as a sacrificial electron donor. Electron injection from the $BiVO_4$ into the p-silicon is clearly observed to occur and to result in a maximum photovoltage of 150 mV for a 1650 nm thick film under 0.3 mW cm^{-2} illumination at 3.5 eV. This establishes the $BiVO_4$−p-Si interface as a tandem-like junction. Charge separation in the $BiVO_4$ film is limited by light absorption and by slow electron transport to the Si interface, based on time-dependent SPS measurements. These problems need to be overcome in functional tandem devices for photoelectrochemical water oxidation.

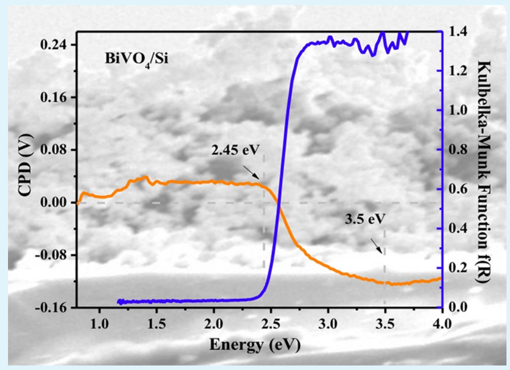

KEYWORDS: *tandem, z-scheme, water splitting, surface photovoltage spectroscopy, photoelectrochemistry, photocatalyst*

INTRODUCTION

Tandem junctions between two semiconductors are of interest for the conversion of solar into electrical and chemical energy.[1−5] Connecting two light absorbers in series increases the open circuit voltage of the photovoltaic cell and its performance, especially when the semiconductors absorb light in different ranges of the solar spectrum. This is important for water splitting cells, which require open circuit voltages in excess of 1.23 V.[6−10] Most of the tandem junctions studied to date consist of well-defined interfaces fabricated by vapor deposition techniques.[11−13] For example, Shaner et al. reported a n-p(+)-Si/n-WO_3 microwire junction obtained by successive vacuum deposition of BCl_3 to achieve Si p-doping, DC sputter coating of an ITO ohmic contact, and electrodeposition of n-WO_3, followed by annealing at 400 °C for 2 h. The device supported overall water splitting with 0.0019% solar to hydrogen (STH) efficiency.[12] Recently, there is also increasing interest in tandem junctions formed between suspended semiconductor particles. Such tandem or "z-scheme photocatalysts" usually employ soluble redox couples for charge transfer.[4,14−17] This is necessary because the rough surfaces of the particles preclude controlled charge transfer between the subsystems. In rare cases the redox couple can be eliminated.[18] For example, mixing of Rh:$SrTiO_3$ and $BiVO_4$ particle suspensions at pH 3.5 produces a junction that supports overall water splitting with quantum yields of up to 4.2% at 420 nm and STH efficiency of 0.1%.[18,19] However, the details of the electrical contact and the effects of water and electrolytes on its function are not well understood. In general, junctions between particles are difficult to probe with electrochemical techniques, due to screening effect from electrolytes and due to the slow charge transport in particulate films. Photocurrents for particulate electrodes generally do not exceed a few microamperes per square centimeter because of the large film resistance and because of poor redox kinetics at the solid−liquid interface.[20−22] The resulting potential drops obscure the photovoltage at the particle junctions and complicate the data interpretation. Here we employ surface photovoltage spectroscopy (SPS) to overcome this problem and to shed light on photochemical charge transfer between particulate light absorbers. SPS is a highly sensitive technique[23] for the observation of photochemical charge transfer at nanoscale junctions.[24−26] Because the method relies on potential changes, not currents, it can probe individual junctions without the need for a coupled redox system.[27,28] As initial target system we choose the combination of bismuth vanadate ($BiVO_4$) and p-silicon. Bismuth vanadate has recently emerged as a promising photocatalyst for the water oxidation reaction.[11,29] The material

Received: January 9, 2015
Accepted: February 20, 2015
Published: February 20, 2015

DOI: 10.1021/acsami.5b00257
ACS Appl. Mater. Interfaces 2015, 7, 5959−5964

has a bandgap of 2.4 eV, but its conduction band edge is located just short of the thermodynamic proton reduction potential, making it unsuitable for overall water splitting.[30−34] This disadvantage can be overcome by connecting n-$BiVO_4$ in series with a p-Si as a photocathode. Silicon photocathodes have been shown to support proton reduction at up to 10 mA cm^{-2} at 0.20 V underpotential, after addition of Pt or MoS_2 cocatalysts,[35,36] and single crystalline silicon absorbers can generate up to 0.71 V photovoltage.[37] As we show here, thin films of n-$BiVO_4$ on an aluminum-doped silicon wafer can be obtained by simple drop-coating of the $BiVO_4$ particle suspensions, followed by thermal annealing at 80 °C. Surface photovoltage spectra (SPS) of the films prove electron injection from the illuminated $BiVO_4$ layer into Si and photovoltages of up to 0.15 V generated at the junction, even under low intensity illumination (<10 mW cm^{-2}). This voltage is close to the theoretical limit for this material combination. The voltage increase by 44 mV in the presence of absorbed methanol is consistent with hole injection from $BiVO_4$ into this sacrificial electron donor. This confirms the functionality of the system as a photoelectrochemical tandem junction. Overall, these results shed new light on photochemical charge transfer between metal oxide and main group element absorbers. They are relevant to the design of future low cost particle-based tandem and z-scheme solar energy conversion devices.

■ RESULTS AND DISCUSSION

The $BiVO_4$ particles for this study were prepared from Bi_2O_3 and VO_2, as described previously,[26,38] and their structure and optical properties were confirmed by XRD and diffuse reflectance spectroscopy (Supporting Information Figure S1). According to TEM, the particles are irregularly shaped and have an average size of 81 nm ± 34 nm. Tauc plots (Figure S1d, Supporting Information) yield indirect and direct band gaps of 2.45 and 2.57 eV, respectively, similar to previous reports.[30] Thin films of n-$BiVO_4$ on aluminum-doped p-type Si wafers or FTO substrates (Figure 1) were obtained by drop-coating

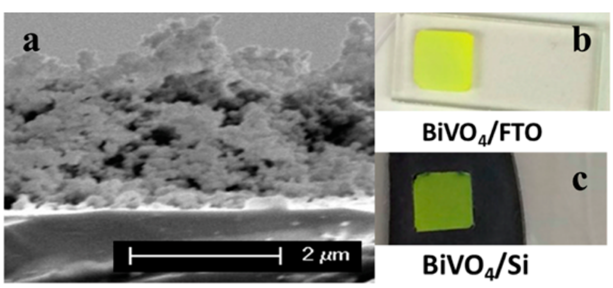

Figure 1. (a) Cross-section of $BiVO_4$ on a Si wafer. Photos of $BiVO_4$ on FTO (b) and Si (c).

$BiVO_4$ particle suspensions in water, followed by drying and mild heating to 80 °C. The $BiVO_4$ particle films extend over an area of approximately 0.68 cm^2 and have thicknesses between 295 and 3398 nm, according to profilometry (Figure S2 and S3, Supporting Information). The thickness of the films can be adjusted with the particle concentration, as described in Experimental Section. According to the SEM in Figure 1, particles in the films are partially aggregated and the films are porous (Figure 1).

Figure 2 shows surface photovoltage spectra of a p-Si wafer, for films of $BiVO_4$ on FTO and silicon, and optical absorbance data. The p-Si wafer alone produces a positive ΔCPD signal

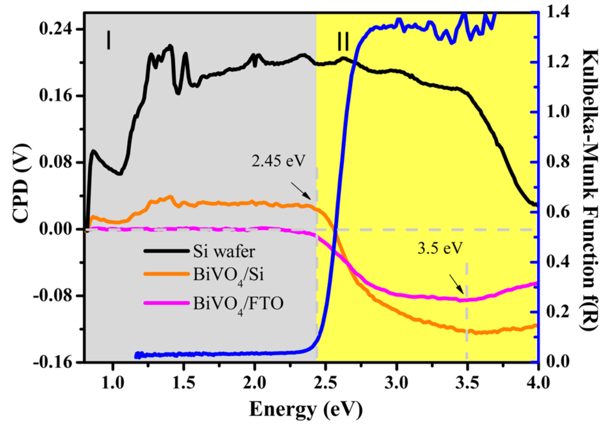

Figure 2. Surface photovoltage spectra of a Si wafer and 600 nm $BiVO_4$ films coated on FTO and a Si wafer. Regions I and II refer to the absorption of silicon and $BiVO_4$, respectively. The optical absorbance spectrum of a $BiVO_4$ film on FTO is also shown.

when the illumination energy exceeds 0.8 eV, close to the indirect band gap of silicon (1.12 eV). The maximum ΔCPD signal of ca. 0.2 V occurs between 1.26 and 3.5 eV. The voltage sign is positive, in agreement with previous SPS studies on this material.[39] The sign of the photovoltage can be understood on the basis of the depleted semiconductor surface model, where band bending at the Si surface is caused by surface states (Figure 3a).[27,40] This interpretation is confirmed by the SPV

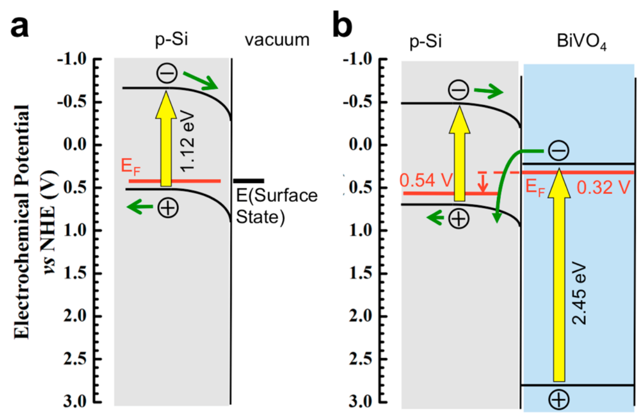

Figure 3. (a) Energy diagram for depleted p-Si surface as a result of surface states (compare Kronik et al.[27,40]). (b) Energy diagram of n-$BiVO_4$/p-Si configuration. The Fermi level of $BiVO_4$ is 0.32 eV,[26] while the Fermi level of p-Si is 0.54 eV, based on photo-electrochemistry (Figure S6, Supporting Information) and Kelvin probe measurements.[44]

spectrum of a n-type wafer which produces an identical photovoltage spectrum but with opposite polarity (Figure S4, Supporting Information). Above 1.1 eV, the SPV spectrum shows a fine structure with peaks occurring at 1.25 and 1.4 eV. These peaks are an artifact of the measurement system and can be attributed to the characteristic Xe emission lines of the light source (Figure S5, Supporting Information). Coating of the wafer with a $BiVO_4$ particle film causes several changes of the SPV spectrum, as shown in Figure 2. First, the positive Si photovoltage at energies below 2.45 eV is reduced from +0.19 V to +0.03 V. This is attributed to the light scattering effect of the porous $BiVO_4$ layer, which reduces the amount of photons that can excite the silicon wafer. In addition, the metal oxide

DOI: 10.1021/acsami.5b00257
ACS Appl. Mater. Interfaces 2015, 7, 5959−5964

reduces the band bending at the Si surface by about 60% (Figure 3b and discussion below). Second, the p-Si/n-$BiVO_4$ system contains a new negative photovoltage feature at >2.45 eV (region II), which is due to band gap excitation of n-$BiVO_4$ and electron transfer to silicon. This assignment can be verified by comparison with the optical spectrum of $BiVO_4$ and its SPV spectrum on FTO (Figure 2). While on FTO the maximum photovoltage is −0.083 V at 3.5 eV, on silicon it reaches −0.15 V. This shows that electron injection from $BiVO_4$ into Si is more favorable than electron injection into FTO.

Charge transfer at the p-Si−$BiVO_4$ contact can be understood with the energy scheme in Figure 3b. Based on the difference of Fermi levels, E_f(p-Si) − E_f($BiVO_4$) = 0.54 − 0.32 = 0.22 eV, the driving force for electron transfer from n-$BiVO_4$ to p-Si is 0.22 eV per electron. The experimental photovoltage of −0.15 V comes close to this value. The negative sign of the photovoltage also rules out the possibility of a p-/n-junction at the silicon−$BiVO_4$ interface. The expected band bending for such a junction would repel electrons in $BiVO_4$ from the interface and produce a positive photovoltage. The absence of a n-/p-junction is a consequence of the low carrier concentration in $BiVO_4$ which does not allow an electrochemical equilibrium with p-Si in the dark. This is analogous to the $HCa_2Nb_3O_{10}$/Au contact described previously.[24] The $BiVO_4$/FTO contact is also ohmic. Here the driving force for electron injection is E_f(FTO) − E_f($BiVO_4$) = 0.56 (±0.1)[41] − 0.32 = 0.24 (±0.1) eV. The observed photovoltage of −0.083 V is much lower. This is attributed decreased physical contact resulting from the high surface roughness of FTO,[42] or due to specific ion absorption.[43]

To obtain additional insight into the factors that govern photochemical charge separation in the p-Si−$BiVO_4$ system, SPV spectra were recorded for $BiVO_4$ films of variable thickness (Figure 4). It can be seen that the Si photovoltage (region I) diminishes with increasing $BiVO_4$ thickness, likely as a result of light scattering by the porous $BiVO_4$ film. Based on optical transmission spectra in Figure S7, Supporting Information, the optical scattering coefficient τ of the porous $BiVO_4$ film can be estimated as 0.072 μm^{-1} at 2 eV. This means that the thinnest $BiVO_4$ film (295 nm) only blocks about 2% of the incoming 2.0 eV photons which cannot explain the significant photovoltage decrease from +0.19 V (at 2.0 eV from Figure 2) for the uncoated silicon wafer to +0.07 V (at 2.0 eV) for the 295 nm $BiVO_4$ film). Instead, the observed 0.12 V (63%) photovoltage reduction is attributed to a decrease of the band bending at the Si surface, as shown in Figure 3b. Such a reduction would be expected from modification or elimination of Si surface states during coating with $BiVO_4$. The dependence of the photovoltage in region II on the thickness of the $BiVO_4$ particle layer is shown in Figure 4b. The photovoltage first rises with $BiVO_4$ thickness to reach a maximum of −0.15 V for the 1650 nm film and then decreases to nearly zero for the thickest film. This trend can be understood in terms of the finite light absorption depth and electron diffusion length of $BiVO_4$. The light absorption depth of $BiVO_4$ can be estimated as 250 nm using the reported absorption coefficient of 40 000 cm^{-1} at 420 nm.[45] That means a 750 nm thick $BiVO_4$ film absorbs >95% of the incident super band gap photons. Experimentally, this situation is approached for the 1652 nm thick film in Figure 4a, which gives the greatest photovoltage. This thickness exceeds 750 nm because of the high porosity of the $BiVO_4$ film. Thicker films absorb slightly more photons, but electron hole pairs are generated further away from the Si/$BiVO_4$ interface, which makes injection into the Si wafer more difficult. Experimental values for the electron diffusion length L_e of $BiVO_4$ films range between 10 and 70 nm depending on technique and preparation.[46,47] This confirms that electron transport becomes the main limitation for the photovoltage, and it explains the observed photovoltage decrease with increasing film thickness as seen in Figure 4b. As expected, the operation of the junction also depends on light intensity. Voltage measurements under illumination with variable light intensity at 420 nm (2.95 eV) are shown in Figure 5a. At this excitation energy, the photovoltage is negative, in agreement with the electron transfer scheme in Figure 3b. For a single junction, the voltage is expected to have a logarithmic dependence on intensity.[24] In the experiments we observe a slightly parabolic dependence (Figure 5b), which indicates that additional factors, such as light absorption, play a role. From Figure 5a, it can be seen that it takes up to 10 min for the voltage to reach a steady state. This suggests that electron transport in the $BiVO_4$ film is slow and limited by diffusion. Indeed, a plot of the photovoltage change rate d(CPD)/dt versus the light power P (Figure S8, Supporting Information) is linear, as expected for a diffusion controlled process.

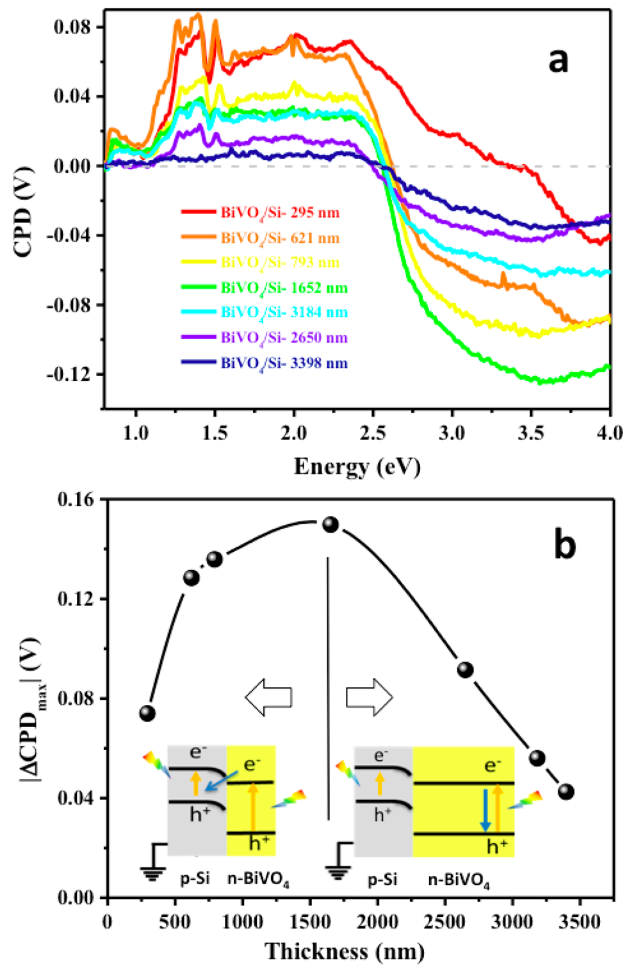

Figure 4. (a) Surface photovoltage spectra of $BiVO_4$−Si junction with variable $BiVO_4$ thickness (thermal annealing at 80 °C). (b) Peak photovoltage (ΔCPD_{max}) at 3.5 eV versus thickness.

Lastly, we probe the ability of the junction to promote electrochemical oxidation of a sacrificial electron donor. For this purpose, p-Si−$BiVO_4$ films are exposed briefly to methanol vapor before the SPS scan is performed under vacuum (Figure 6), using the same procedure as previously reported for a

DOI: 10.1021/acsami.5b00257
ACS Appl. Mater. Interfaces 2015, 7, 5959−5964

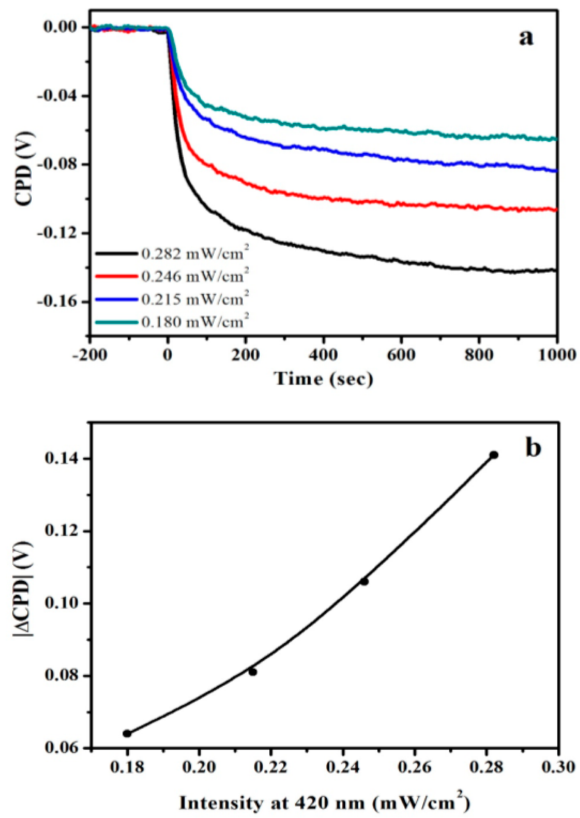

Figure 5. (a) Photovoltage responses of $BiVO_4$ on a Si wafer (thickness ca. 1652 nm) under monochromatic illumination with variable intensity (0.180–0.282 mW/cm^2 at 420 nm, 2.95 eV. (b) Plot of ΔCPD versus the intensity from a.

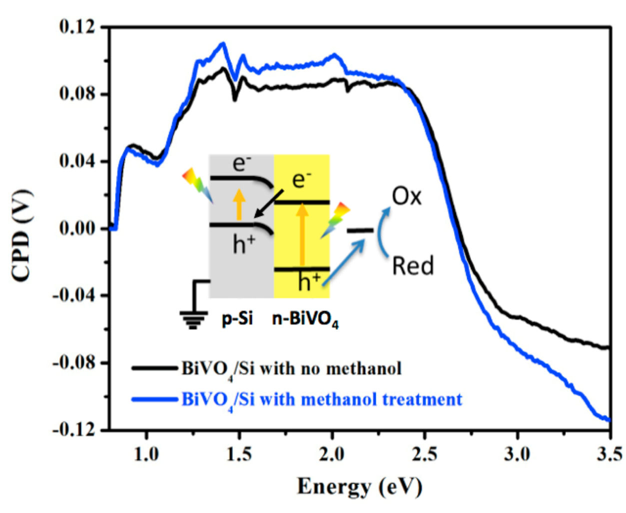

Figure 6. Photovoltage spectra of $BiVO_4$ on a p-Si wafer in vacuum before and after treatment with methanol vapor.

$HCa_2Nb_3O_{10}$ nanocrystal film.[24] We find that methanol exposure does increase the photovoltage at 3.5 eV by 0.044 V. This confirms that photogenerated holes in $BiVO_4$ can transfer to methanol. Interestingly, methanol vapor treatment also increases the positive photovoltage in region I. This indicates that the adsorbed methanol molecules either reduce the optical scattering characteristics of the porous $BiVO_4$ film or cause a further change of the surface band bending in silicon.

CONCLUSION

We present the first study of photochemical charge transport at a p-Si–$BiVO_4$ particle junction made by physical assembly. The data confirms that that the components form a functional tandem or "z-scheme" type junction. Surface photovoltage spectroscopy confirms the ability of the junction to separate charge, oxidize methanol, and generate a photovoltage close to the theoretical limit, as defined by the work functions of the components. However, the function of the tandem junction is limited by slow electron transport through the $BiVO_4$ layer and by the need for thick films to absorb all super bandgap photons. Also we find that the p-Si–$BiVO_4$ particle films are too mechanically unstable to be used as a photoelectrode in an electrochemical cell. These problems need to be overcome in tandem junctions for the conversion of photochemical into electrical or chemical energy.

EXPERIMENTAL SECTION

Chemicals. Bismuth(III) oxide (99.9999% Acros Organics) and vanadium(IV) oxide (99+% Strem Chemicals) were used as received. Acetic acid (glacial, Macron) and nitric acid (68–70%, EMD) were used after dilution. Water was purified to 18 MΩ·cm resistivity by a Nanopure II system. Al-doped (~10^{15} cm^{-3}) silicon wafers with a resistivity of 10–100 Ω·cm were purchased from WRS Materials.

$BiVO_4$ Synthesis. $BiVO_4$ was synthesized via a revised solid–solution method.[26] At room temperature, 1.15 g (2.5 mmol) of Bi_2O_3 and 0.42 g (5 mmol) of VO_2 were stirred in 25 mL of 1.0 M aqueous acetic acid solution for 11 days. The obtained powder was washed first with water and then with 0.5 M nitric acid and again with water. The washed powder was vacuum-dried and calcined at 673 K for 5 h in air.

Film Preparation. Fluorine-doped tin oxide (FTO) substrates were sonicated sequentially in acetone, methanol and 2-propanol, rinsed with water, and dried in air before use. Silicon wafers were sonicated in acetone, ethanol, and water and then washed with 10% HF solution. After a rinse with pure water, they were dried in air. Films of $BiVO_4$ were prepared by applying various concentrations of $BiVO_4$ dispersions onto 0.8 × 0.8 cm^2 FTO or Si wafers, followed by drying at room temperature for 12 h and annealing at 353 K for 1 h. The resulting films have a thickness ranging between 295 and 3398 nm (Figures S2 and S3, Supporting Information). In the photoxidation experiment, a $BiVO_4$–Si film was exposed to saturated methanol vapor for 5 min and then dried at 353 K for 1 h.

Characterization. Scanning electron microscopy (SEM) images of $BiVO_4$–Si films were obtained on a FEI XL30 high-resolution scanning electron microscope with an operating voltage at 5 kV. UV–vis diffuse reflectance spectra were recorded on a Thermo Scientific Evolution 220 UV–vis spectrometer equipped with an integrating sphere. The reflectance data were converted to the Kubelka–Munk function by $f(R) = (1 - R)^2/(2R)$ and plotted versus energy. Film thickness was measured by a Veeco Dektak profilometer.

Surface Photovoltage Spectroscopy (SPS). SPS measurements were conducted using a vibrating gold Kelvin probe (3 mm diameter, Delta PHI Besocke) mounted inside a home-built vacuum chamber (<1 × 10^{-4} mbar). The distance between sample and gold probe is 1 mm. Samples were illuminated with monochromatic light (1–10 mW·cm^{-2}) generated by a Cornerstone 130 monochromator behind a 150 W Xe arc lamp. A typical photovoltage spectrum was recorded by monitoring the contact potential difference (CPD) during a monochromatic scan from 0.8 to 4 eV (1550 to 310 nm). Time-dependent photovoltage measurements were performed with 2.95 eV (420 nm) light of variable power. All surface photovoltage spectra were corrected for drift effects by subtracting dark scan background.

DOI: 10.1021/acsami.5b00257
ACS Appl. Mater. Interfaces 2015, 7, 5959–5964

ASSOCIATED CONTENT

Supporting Information

Additional characterization, optical, and photoelectrochemical data. This material is available free of charge via the Internet at http://pubs.acs.org.

AUTHOR INFORMATION

Corresponding Author

*E-mail: fosterloh@ucdavis.edu. Tel: +1 530-754-6242. Fax: +1-530-752-8995.

Notes

The authors declare no competing financial interest.

ACKNOWLEDGMENTS

We thank Adam Moulé for access to his profilometer and Joshua Greenfield and Kirill Kovnir for XRD data. We are grateful for financial support from Research Corporation for Science Advancement (Scialog Award) and from the National Science Foundation (NSF, grants 1152250 and 1133099). Y.Y. thanks the Natural Science Fund Council of China (51478097, 51178092, 51278092, 21173036) for support.

REFERENCES

(1) Osterloh, F. E. Inorganic Nanostructures for Photoelectrochemical and Photocatalytic Water Splitting. *Chem. Soc. Rev.* **2013**, *42*, 2294−2320.

(2) Nozik, A. J. Photochemical Diodes. *Appl. Phys. Lett.* **1977**, *30*, 567−569.

(3) Khaselev, O.; Turner, J. A. A Monolithic Photovoltaic-Photoelectrochemical Device for Hydrogen Production via Water Splitting. *Science* **1998**, *280*, 425−427.

(4) Kudo, A. Z-Scheme Photocatalyst Systems for Water Splitting under Visible Light Irradiation. *MRS Bull.* **2011**, *36*, 32−38.

(5) Chang, L.; Holmes, M. A.; Waller, M.; Osterloh, F. E.; Moule, A. J. Calcium Niobate Nanosheets as Novel Electron Transport Material for Solution-processed Multi-junction Polymer Solar Cell. *J. Mater. Chem.* **2012**, *22*, 20443−20450.

(6) Hu, S.; Xiang, C. X.; Haussener, S.; Berger, A. D.; Lewis, N. S. An Analysis of the Optimal Band Gaps of Light Absorbers in Integrated Tandem Photoelectrochemical Water-Splitting Systems. *Energy Environ. Sci.* **2013**, *6*, 2984−2993.

(7) Ronge, J.; Bosserez, T.; Martel, D.; Nervi, C.; Boarino, L.; Taulelle, F.; Decher, G.; Bordiga, S.; Martens, J. A. Monolithic Cells for Solar Fuels. *Chem. Soc. Rev.* **2014**, *43*, 7963−7981.

(8) Gratzel, M. Mesoscopic Solar Cells for Electricity and Hydrogen Production from Sunlight. *Chem. Lett.* **2005**, *34*, 8−13.

(9) Walter, M. G.; Warren, E. L.; McKone, J. R.; Boettcher, S. W.; Mi, Q. X.; Santori, E. A.; Lewis, N. S. Solar Water Splitting Cells. *Chem. Rev.* **2010**, *110*, 6446−6473.

(10) Krol, R., Principles of Photoelectrochemical Cells. In *Photoelectrochemical Hydrogen Production*, van de Krol, R.; Grätzel, M., Eds.; Springer: New York, 2012; Chapter 2, pp 13−67.

(11) Abdi, F. F.; Han, L. H.; Smets, A. H. M.; Zeman, M.; Dam, B.; van de Krol, R., Efficient Solar Water Splitting by Enhanced Charge Separation in a Bismuth Vanadate-Silicon Tandem Photoelectrode. *Nat. Commun.* **2013**, *4*.

(12) Shaner, M. R.; Fountaine, K. T.; Ardo, S.; Coridan, R. H.; Atwater, H. A.; Lewis, N. S. Photoelectrochemistry of Core-Shell Tandem Junction n-p(+)-Si/n-WO_3 Microwire Array Photoelectrodes. *Energy Environ. Sci.* **2014**, *7*, 779−790.

(13) Coridan, R. H.; Arpin, K. A.; Brunschwig, B. S.; Braun, P. V.; Lewis, N. S. Photoelectrochemical Behavior of Hierarchically Structured Si/WO_3 Core−Shell Tandem Photoanodes. *Nano Lett.* **2014**, *14*, 2310−2317.

(14) Osterloh, F. E. Inorganic Materials as Catalysts for Photochemical Splitting of Water. *Chem. Mater.* **2008**, *20*, 35−54.

(15) Abe, R. Recent Progress on Photocatalytic and Photoelectrochemical Water Splitting under Visible Light Irradiation. *J. Photochem. Photobiol. C* **2010**, *11*, 179−209.

(16) Sayama, K.; Yoshida, R.; Kusama, H.; Okabe, K.; Abe, Y.; Arakawa, H. Photocatalytic Decomposition of Water into H-2 and O-2 by a Two-Step Photoexcitation Reaction Using a WO_3 Suspension Catalyst and an Fe^{3+}/Fe^{2+} Redox System. *Chem. Phys. Lett.* **1997**, *277*, 387−391.

(17) Maeda, K. Z-Scheme Water Splitting Using Two Different Semiconductor Photocatalysts. *ACS Catal.* **2013**, *3*, 1486−1503.

(18) Sasaki, Y.; Nemoto, H.; Saito, K.; Kudo, A. Solar Water Splitting Using Powdered Photocatalysts Driven by Z-Schematic Interparticle Electron Transfer without an Electron Mediator. *J. Phys. Chem. C* **2009**, *113*, 17536−17542.

(19) Kato, H.; Sasaki, Y.; Shirakura, N.; Kudo, A. Synthesis of Highly Active Rhodium-Doped $SrTiO_3$ Powders in Z-Scheme Systems for Visible-Light-Driven Photocatalytic Overall Water Splitting. *J. Mater. Chem. A* **2013**, *1*, 12327−12333.

(20) Maeda, K. Rhodium-Doped Barium Titanate Perovskite as a Stable p-Type Semiconductor Photocatalyst for Hydrogen Evolution under Visible Light. *ACS Appl. Mater. Interfaces* **2014**, *6*, 2167−2173.

(21) Liu, J.; Hisatomi, T.; Ma, G.; Iwanaga, A.; Minegishi, T.; Moriya, Y.; Katayama, M.; Kubota, J.; Domen, K. Improving the Photoelectrochemical Activity of $La_5Ti_2CuS_5O_7$ for Hydrogen Evolution by Particle Transfer and Doping. *Energy Environ. Sci.* **2014**, *7*, 2239−2242.

(22) Joshi, U. A.; Palasyuk, A. M.; Maggard, P. A. Photoelectrochemical Investigation and Electronic Structure of a p-Type $CuNbO_3$ Photocathode. *J. Phys. Chem. C* **2011**, *115*, 13534−13539.

(23) Lagowski, J.; Edelman, P.; Kontkiewicz, A. M.; Milic, O.; Henley, W.; Dexter, M.; Jastrzebski, L.; Hoff, A. M. Iron Detection in the Part Per Quadrillion Range in Silicon Using Surface Photovoltage and Photodissociation of Iron - Boron Pairs. *Appl. Phys. Lett.* **1993**, *63*, 3043−3045.

(24) Zhao, J.; Osterloh, F. E. Photochemical Charge Separation in Nanocrystal Photocatalyst Films − Insights from Surface Photovoltage Spectroscopy. *J. Phys. Chem. Lett.* **2014**, *5*, 782−786.

(25) Osterloh, F. E.; Holmes, M. A.; Zhao, J.; Chang, L.; Kawula, S.; Roehling, J. D.; Moulé, A. J. P3HT:PCBM Bulk-Heterojunctions: Observing Interfacial and Charge Transfer States with Surface Photovoltage Spectroscopy. *J. Phys. Chem. C* **2014**, *118*, 14723−14731.

(26) Wang, J.; Osterloh, F. E. Limiting Factors for Photochemical Charge Separation in $BiVO_4/Co_3O_4$, a Highly Active Photocatalyst for Water Oxidation in Sunlight. *J. Mater. Chem. A* **2014**, *2*, 9405−9411.

(27) Kronik, L.; Shapira, Y. Surface Photovoltage Spectroscopy of Semiconductor Structures: At the Crossroads of Physics, Chemistry and Electrical Engineering. *Surf. Interface Anal.* **2001**, *31*, 954−965.

(28) Lagowski, J. Semiconductor Surface Spectroscopies - The Early Years. *Surf. Sci.* **1994**, *299*, 92−101.

(29) Kudo, A.; Ueda, K.; Kato, H.; Mikami, I. Photocatalytic O-2 Evolution under Visible Light Irradiation on $BiVO_4$ in Aqueous $AgNO_3$ Solution. *Catal. Lett.* **1998**, *53*, 229−230.

(30) Park, Y.; McDonald, K. J.; Choi, K. S. Progress in Bismuth Vanadate Photoanodes for Use in Solar Water Oxidation. *Chem. Soc. Rev.* **2013**, *42*, 2321−2337.

(31) He, H.; Berglund, S. P.; Rettie, A. J. E.; Chemelewski, W. D.; Xiao, P.; Zhang, Y.; Mullins, C. B. Synthesis of $BiVO_4$ Nanoflake Array Films for Photoelectrochemical Water Oxidation. *J. Mater. Chem. A* **2014**, *2*, 9371−9379.

(32) Hong, S. J.; Lee, S.; Jang, J. S.; Lee, J. S. Heterojunction $BiVO_4$/WO_3 Electrodes for Enhanced Photoactivity of Water Oxidation. *Energy Environ. Sci.* **2011**, *4*, 1781−1787.

(33) Pilli, S. K.; Furtak, T. E.; Brown, L. D.; Deutsch, T. G.; Turner, J. A.; Herring, A. M. Cobalt-Phosphate (Co-Pi) Catalyst Modified Mo-Doped $BiVO_4$ Photoelectrodes for Solar Water Oxidation. *Energy Environ. Sci.* **2011**, *4*, 5028−5034.

(34) Prévot, M. S.; Sivula, K. Photoelectrochemical Tandem Cells for Solar Water Splitting. *J. Phys. Chem. C* **2013**, *117*, 17879−17893.

(35) Hou, Y.; Abrams, B. L.; Vesborg, P. C. K.; Björketun, M. E.; Herbst, K.; Bech, L.; Setti, A. M.; Damsgaard, C. D.; Pedersen, T.;

Hansen, O.; Rossmeisl, J.; Dahl, S.; Nørskov, J. K.; Chorkendorff, I. Bioinspired Molecular Co-Catalysts Bonded to a Silicon Photocathode for Solar Hydrogen Evolution. *Nat. Mater.* **2011**, *10*, 434−438.

(36) Boettcher, S. W.; Warren, E. L.; Putnam, M. C.; Santori, E. A.; Turner-Evans, D.; Kelzenberg, M. D.; Walter, M. G.; McKone, J. R.; Brunschwig, B. S.; Atwater, H. A.; Lewis, N. S. Photoelectrochemical Hydrogen Evolution Using Si Microwire Arrays. *J. Am. Chem. Soc.* **2011**, *133*, 1216−1219.

(37) Osterloh, F. E. Maximum Theoretical Efficiency Limit of Photovoltaic Devices: Effect of Band Structure on Excited State Entropy. *J. Phys. Chem. Lett.* **2014**, 3354−3359.

(38) Iwase, A.; Kudo, A. Photoelectrochemical Water Splitting Using Visible-Light-Responsive $BiVO_4$ Fine Particles Prepared in an Aqueous Acetic Acid Solution. *J. Mater. Chem.* **2010**, *20*, 7536−7542.

(39) Burstein, L.; Shapira, Y.; Partee, J.; Shinar, J.; Lubianiker, Y.; Balberg, I. Surface Photovoltage Spectroscopy of Porous Silicon. *Phys. Rev. B* **1997**, *55*, R1930−R1933.

(40) Kronik, L.; Shapira, Y. Surface Photovoltage Phenomena: Theory, Experiment, and Applications. *Surf. Sci. Rep.* **1999**, *37*, 1−206.

(41) Helander, M. G.; Greiner, M. T.; Wang, Z. B.; Tang, W. M.; Lu, Z. H. Work function of fluorine doped tin oxide. *J. Vac. Sci. Technol. A* **2011**, *29*, 011019.

(42) Le Formal, F.; Gratzel, M.; Sivula, K. Controlling Photoactivity in Ultrathin Hematite Films for Solar Water-Splitting. *Adv. Funct. Mater.* **2010**, *20*, 1099−1107.

(43) Chamousis, R. L.; Osterloh, F. E. Use of Potential Determining Ions to Control Energetics and Photochemical Charge Transfer of a Nanoscale Water Splitting Photocatalyst. *Energy Environ. Sci.* **2014**, *7*, 736−743.

(44) Novikov, A. Experimental measurement of work function in doped silicon surfaces. *Solid-State Electron.* **2010**, *54*, 8−13.

(45) Zhong, D. K.; Choi, S.; Gamelin, D. R. Near-Complete Suppression of Surface Recombination in Solar Photoelectrolysis by "Co-Pi" Catalyst-Modified W:$BiVO_4$. *J. Am. Chem. Soc.* **2011**, *133*, 18370−18377.

(46) Abdi, F. F.; Savenije, T. J.; May, M. M.; Dam, B.; van de Krol, R. The Origin of Slow Carrier Transport in $BiVO_4$ Thin Film Photoanodes: A Time-Resolved Microwave Conductivity Study. *J. Phys. Chem. Lett.* **2013**, *4*, 2752−2757.

(47) Seabold, J. A.; Zhu, K.; Neale, N. R. Efficient Solar Photoelectrolysis by Nanoporous Mo:$BiVO_4$ Through Controlled Electron Transport. *Phys. Chem. Chem. Phys.* **2014**, *16*, 1121−1131.

DOI: 10.1021/acsami.5b00257
ACS Appl. Mater. Interfaces 2015, 7, 5959−5964